Power sizing of wireless power systems feeding in-motion electric vehicles at constant power

Giuseppe Buja[1], *Life Fellow, IEEE*, Rupesh Jha[2], Manuele Bertoluzzo[1]*, and Ritesh Keshri[3], *Senior member, IEEE*,
[1]Department of Industrial Engineering, University of Padova, Padova, Italy, [2]Zeal College of Engineering and Research, Pune, India, [3]Department of Electrical Engineering, Visvesvaraya National Institute of Technology, India
*Corresponding author: manuele.bertoluzzo@unipd.it

***Abstract* –The paper is concerned with the wireless power (WP) systems feeding in-motion electric vehicles (EVs) and focuses on the power sizing of three key WP system components, namely the track coils, the pickup and the voltage supply. It is assumed that the track is made of lumped type with no overlapped coupling of the pickup, and that the track coils and the pickup are compensated for by series resonating capacitors. Power sizing equations are formulated for a WP system that is controlled in the way of transferring a constant power to EVs during their motion over a large part of the track coils. Due to the variation of the coupling between the pickup and a track coil, the transfer of a constant power requires the adjustment of the currents in the WP system, obtained by commanding the embedded power conversion units. Two solutions are examined: by one solution, the pickup side current is controlled at a proper value whilst the track side current is regulated at a constant level; by the other solution, the opposite occurs. Power sizing equations are expressed in terms of specifications and parameters of the WP system. The equations outline that the power sizing is higher for the components in the side where the current control is executed. At last, the case study of a WP system is examined, showing the convenience of the track-side control.**

Index Terms—Wireless power transfer, Electric vehicles (EVs), In-motion EV wireless charging.

I. INTRODUCTION

Wireless power (WP) transfer [1], [2] is a feasible technology to feed the propulsion drive of the in-motion electric vehicles (EVs), leaving to the battery the task of acting as an energy buffer. From this perspective, the WP systems play the role of WP feeders (WPFs) of EVs rather than of WP rechargers of their battery.

Out of some WP transfer technologies, that one based on the inductive coupling is the most convenient for WPFs [3], with the transmitting coils, denoted as track, buried under the road surface and the receiving coil, denoted as pickup, mounted on the EV flatbed [4], [5]. Track coils and pickup are two key WPF components. To remedy the absorption of reactive power by the track coils and the pickup, they are supplemented with reactive compensation networks.

WPF tracks are either stretched or lumped [6]. Coils of the stretched tracks are somewhat longer than the pickup and the mutual inductance between the pickup and a track coil is constant and equal to the maximum value for most of the coupling interval, which is the interval along the EV route where the pickup has a non-zero mutual inductance with a track coil. Instead, coils of the lumped tracks have a length comparable with the pickup so that the mutual inductance between the pickup and a track coil is varying from zero to a maximum and again to zero along the coupling interval, with no or a very short interval where it is constant at the maximum value. Lumped tracks exhibit some merits over the stretched ones, like higher efficiency, and are hereafter considered [7], [8].

Another key component of WPFs is the voltage supply on the track side. It consists of a high-frequency (HF) voltage inverter whose output frequency is kept constant at many tens of kHz and whose output voltage magnitude is commanded by the phase-shift technique. HF inverter is one of the two power conversion units with control capabilities embedded in WPFs. The other one is the ac-dc converter located on the pickup side; it consists of the cascade of a diode rectifier (DR) and a chopper that definitively feds EV at the requested voltage level.

Variation of the mutual inductance between the pickup and a track coil during the EV motion affects the transferred power, with the shortcomings of a low exploitation of the WPF circuitry and a fluctuation of the power feeding EV. Indeed, with no any intervention, the nominal power is transferred from a track coil to the pickup in correspondence of the maximum of the mutual inductance, which commonly takes place when the pickup is aligned to the track coil, while it drops as soon as the pickup is situated before or after the alignment condition. To overcome the above-mentioned shortcomings, some countermeasures are taken. They are based on a suitable design of the compensation networks, which is carried out by means of two approaches. One approach is directed at minimizing the sensitivity of the transferred power to the variation of the mutual inductance [8]-[10]. The other one is directed at levelling the transferred power by extending the transfer of the nominal power in an interval around the alignment condition. [11]-[13]. These approaches are implemented by means of complex reactive compensation networks, often made of two or even three elements, that increase the cost of WPFs and impair their efficiency because of the losses in the parasitic resistances of the added elements; furthermore, the latter approach requests the oversizing of the WPF circuitry in terms of either voltage or current or both to reach the levelling objective.

In this paper, a workaround to the above-mentioned shortcomings is presented that, differently from the existing countermeasures, is aimed at keeping constant the transferred power along a large part of the coupling interval by adapting the WPF currents. In the paper, such a part of the interval is designated with WPF operating interval. Two solutions are

examined: by the first solution, the current in the pickup side is controlled by commanding the ac-dc converter while the current in the track side is regulated at a constant level; by the second solution, the current is controlled in the track side by commanding the HF inverter while the current in the pickup side is regulated at a constant level. For the two solutions, the power sizing of the three key WPF components: track coils, pickup and voltage supply, are formulated as a function of the nominal power drawn by EV, the EV DC bus voltage and the WPF inductive parameters, including the mutual inductances at the edges of the WPF operating range.

Organization of the paper is as follows. Section II describes the WPF circuitry, sets the basic relationships for the WPF voltages and currents, and defines dimensionless quantities for the power sizing, termed as power sizing factors. Sections III and IV deal with the control of the current in the pickup side and in the track side, respectively, and formulate the power sizing factors for the three key WPF components. Section V discusses the findings of the previous Sections and supports the discussion with the results obtained for a WPF case study. Section VI concludes the paper. Appendix reports the data of the case study.

Throughout the paper, upper-case letters denote WPF elements or rms values of sinusoidal quantities; the same letters with a bar on denote phasor quantities; subscripts N, M and m stay respectively for nominal, maximum and minimum values of the quantities.

II. WPF BACKGROUND

A) Description

The circuital diagram of WPF for EV is illustrated in Fig. 1 (a) and is comprised of two sides: track and pickup, which are distinguished by subscripts t and p of the relevant components and quantities.

The coupler, i.e. the coil set formed by a track coil and the pickup, is represented by coil self-inductances L_t and L_p, mutual coil inductance M, emfs V_t and V_p induced in the coils, and coil terminal voltages V_{tt} and V_{pt}. The coil inductances are compensated for by series resonating capacitors C_t and C_p, and are flowed by current I_t and I_p. Output voltage of the HF inverter supplying WPF is denoted with V_s while the input voltage of the WPF load is denoted with V_l.

The diagram of the WPF load is illustrated in Fig. 1 (b), where C_{DR} is the filtering capacitor at the DR output, V_{CH} is the chopper input voltage and I_{CH} is the average chopper input current. The output of the chopper is connected to the EV DC bus; voltage and current at the chopper output are denoted with V_V and I_V. Let us presume that the EV battery is connected to the DC bus and its nominal voltage be V_B; then, the following relation holds: $V_{VN}=V_B$. Current I_V, in turn, is the sum of current I_D absorbed by the EV propulsion drive and current I_B absorbed by the battery; its nominal value I_{VN} is given by

$$I_{VN} = \frac{P_{VN}}{V_B} \tag{1}$$

where P_{VN} is the nominal power drawn by EV.

The analysis of the WPF circuital diagram is accomplished for a lumped track under the usual assumptions of i) sinusoidal approximation of the alternate quantities in Fig. 1 (a); as a matter of fact: currents and, then, emfs are nearly sinusoidal due to the filtering action of the LC branches, so that only the fundamental components of the supply and load voltages, which have a square-type waveshape, determine the power flow within WPF, ii) continuous DR conduction, iii) triangular profile of M along the EV motion with no overlapped coupling between the pickup and two successive track coils, as sketched in Fig. 2 where x is the EV motion axis and D is the coupling interval, and iv) constant value of V_B.

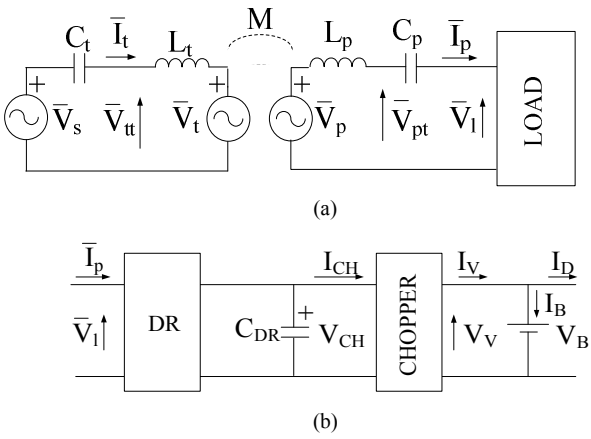

Fig. 1. (a) WPF circuital diagram, (b) Load block diagram.

Power sizing of the three key WPF components is formulated for EV drawing a constant power equal to nominal value P_{VN} in the WPF operating range. Since the losses in the WPF circuitry do not affect significantly the power sizing of the components, they are disregarded. Note that, further to this assumption, the active power flowing through all the sections of WPF is P_{VN}.

B) Basic equations

Emfs induced in the coupler are

$$\begin{cases} \bar{V}_p = -j\omega M \bar{I}_t \\ \bar{V}_t = j\omega M \bar{I}_p \end{cases} \tag{2}$$

where ω is the supply angular frequency, and the terminal coil voltages are

$$\bar{V}_{pt} = \bar{V}_p - j\omega L_p \bar{I}_p \tag{3}$$

$$\bar{V}_{tt} = \bar{V}_t + j\omega L_t \bar{I}_t \tag{4}$$

The WPF series-series resonant compensation implies that i) $\bar{V}_p$ and $\bar{V}_l$ as well as $\bar{V}_s$ and $\bar{V}_t$ have the same magnitude and are in phase, i.e. it is

$$\bar{V}_p = \bar{V}_l \tag{5}$$

$$\bar{V}_s = \bar{V}_t \tag{6}$$

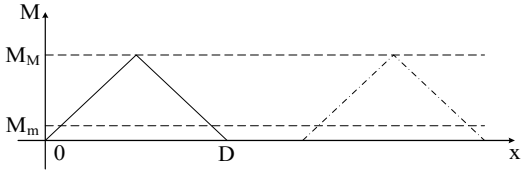

Fig. 2. Mutual inductance along the EV route.

ii) current $\bar{I}_p$ is in phase with both $\bar{V}_p$ and $\bar{V}_l$, and iii) current $\bar{I}_t$ is in phase with both $\bar{V}_s$ and $\bar{V}_t$.

Because of the continuous DR conduction, voltages and currents at the DR input and output are related by

$$V_l = aV_{CH} \tag{7}$$

$$I_p = \frac{I_{CH}}{a} \tag{8}$$

where $a = 2\sqrt{2}/\pi$.

Transfer of some power at very low value of M is not practical as it would require huge values of voltage/current; then the WPF operating range for the power transfer goes from a minimum value of M, denoted with M_m, up to the maximum value, denoted with M_M, as illustrated to in Fig. 2.

C) Power sizing factors

Later one, power sizing values are helpfully expressed in terms of dimensionless factors, given by the ratios of the power sizing to P_{VN}.

Power sizing factors s_{Lt} and s_{Lp} of a track coil and the pickup are defined as the product of the maximum voltage at their terminals by the maximum current flowing into/out the terminals; then s_{Lt} and s_{Lp} are expressed as

$$s_{Lt} = \frac{\max[V_{tt}]\max[I_t]}{P_{VN}} \tag{9}$$

$$s_{Lp} = \frac{\max[V_{pt}]\max[I_p]}{P_{VN}} \tag{10}$$

where max [·] stands for the maximum of the argument when M varies from M_m to M_M. Power sizing factor s_s of the voltage supply is defined in a similar way as

$$s_s = \frac{\max[V_s]\max[I_t]}{P_{VN}} \tag{11}$$

where V_s is the magnitude of the fundamental component of the voltage at the HF inverter output.

D) Power conversion unit command

By realizing from (2) that emfs are current-controlled quantities, it follows that a constant power flow through WPT in the presence of variations of M can be reached only by adjusting the currents in the two sides. This can be done by commanding the HF inverter in the track side and the chopper in the pickup side.

Regarding the chopper, first equation in (2) prompts the use of a boost topology since emf V_p is low at M_m, whilst it is reasonable that V_B is higher than the value of V_{CH} ensuing from the actual magnitude of V_p, as derived by (5) and (7). Moreover, it appears useful (and here pursued) that the chopper is idle when the maximum of V_{CH} equates the battery voltage, i.e. when

$$V_{CHM} = V_B \tag{12}$$

III. PICKUP-SIDE CURRENT CONTROL

Let us control the current in the pickup side while keeping the current in the track side constant at nominal value I_{tN}. From (2), voltage V_p gets its maximum value V_{pM} when $M=M_M$. For the chopper to be idle in correspondence with V_{pM}, it follows from (5), (7) and (12) that

$$I_{tN} = \frac{aV_B}{\omega M_M} \tag{13}$$

Then, current I_{tN} must be set at (13).

A) Current and voltage relationhips

Since the supply voltage and current in the track side are in phase, it follows that

$$V_{sN} = \frac{P_{VN}}{I_{tN}} \tag{14}$$

Eqs. (6) and (14) point out that i) under regulation of I_{tN}, the HF inverter generates a constant voltage, and ii) track emf V_t is constant and equal to V_{sN}, i.e. it is

$$V_t = V_{sN} \tag{15}$$

By the second equation in (2) and (4), condition (14) is fulfilled by controlling I_p inversely to M as plotted in Fig. 3. In turn, being I_t constant, voltage V_p increases linearly with M and the product of twos gives P_{VN}. The relevant equations are

$$I_p = \frac{V_{sN}}{\omega M} \tag{16}$$

$$V_p = \omega M I_{tN} \tag{17}$$

Substitution of (13) and (14) into (16) yields

$$I_p = \frac{M_M}{M}\frac{P_{VN}}{aV_B} \tag{18}$$

and the maximum of I_p is obtained for $M=M_m$

$$\max[I_p] = \frac{M_M}{M_m}\frac{P_{VN}}{aV_B} \tag{19}$$

By (8), current I_p is controlled as per (18) by the boosting action of the chopper. Indeed, as soon as M increases, voltage V_p -and hence V_{CH}- also increases proportionally; consequently, the chopper reduces the boost gain and, with it, current I_p since the chopper output voltage is fixed.

B) Power sizing factors

Voltage supply power sizing factor. Voltage supply works at constant voltage and current, equal to the respective nominal values. Thus, sizing factor s_s of the voltage supply is 1, as it can easily deduced from (11) and (14).

Track coil power sizing factor. For the EV bus drawing constant power P_{VN}, the terminal voltage of the track coil is constant and is given by

$$V_{tt} = \sqrt{V_{sN}^2 + (\omega L_t I_{tN})^2} \tag{20}$$

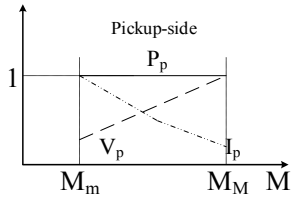

Fig. 3. Pickup current (dashed-dotted line), voltage (dashed line) and power (solid line) profile during pickup-side control. Quantities in the graph are normalized to the respective nominal/maximum values.

By (9), the power sizing factor of the track coil is

$$s_{Lt} = \sqrt{1 + \left(\frac{\omega L_t I_{tN}^2}{P_{VN}}\right)^2} \tag{21}$$

Eq. (21) underlines that s_{Lt} exceeds 1 of a quantity correlated to the reactive power absorbed by L_t. When formulated in terms of P_{VN}, V_B and WPT inductive parameters, by (13), equation (21) becomes

$$s_{Lt} = \sqrt{1 + \left[\frac{L_t}{M_M}\frac{(aV_B)^2}{\omega M_M P_{VN}}\right]^2} \tag{22}$$

Pickup power sizing factor. For the EV bus drawing constant power P_{VN}, by (13) and (17), voltage V_p can be expressed as

$$V_p = \frac{M}{M_M} aV_B \tag{23}$$

Substitution of (18) and (23) into (3) leads to the expression of V_{pt} in (24), which is directly formulated in terms of P_{VN}, V_B and the WPT inductive parameters.

$$V_{pt} = \sqrt{\left(\frac{M}{M_M} aV_B\right)^2 + \left(\frac{M_M}{M}\frac{\omega L_p P_{VN}}{aV_B}\right)^2} \tag{24}$$

Eq. (24) shows that the terminal voltage of the pickup is contributed by two addends that vary in opposite way to M. Then, as a function of M, equation (24) has a bath-tube profile. Taking its derivative with respect to M and equating the result to zero yields

$$M_d = \frac{\omega M_M}{aV_B}\sqrt{\frac{L_p P_{VN}}{\omega}} \tag{25}$$

Since the sign of the derivative is negative for $M<M_d$ and positive for $M>M_d$, voltage V_{pt} is minimum for $M=M_d$. If $M_d>M_M$, i.e. for

$$\frac{\omega L_p P_{VN}}{(aV_B)^2} > 1 \tag{26}$$

voltage V_{pt} reaches the maximum at $M=M_m$; if $M_d<M_m$, i.e. for

$$\frac{\omega L_p P_{VN}}{(aV_B)^2} < \left(\frac{M_m}{M_M}\right)^2 \tag{27}$$

voltage V_{pt} reaches the maximum at $M=M_M$. For $M_m<M_d<M_M$, voltage V_{pt} has relative maxima at the two edges of the M range and the absolute maximum is obtained by inspection. Looking at (26), one recognizes that i) P_{VN} divided by V_B gives I_{VN}, and ii) in practical cases, $\omega L_p I_{VN}$ is greater than aV_B. Then, (26) is supposed to hold and the maximum of V_{pt} is equal to

$$\max[V_{pt}] = \sqrt{\left(\frac{M_m}{M_M} aV_B\right)^2 + \left(\frac{M_M}{M_m}\frac{\omega L_p P_{VN}}{aV_B}\right)^2} \tag{28}$$

By (10), the power sizing factor of the pickup is

$$s_{Lp} = \sqrt{1 + \left(\frac{M_M}{M_m}\right)^4 \left[\frac{\omega L_p P_{VN}}{(aV_B)^2}\right]^2} \tag{29}$$

Eq. (29) underlines that s_{Lp} exceeds 1 of a quantity correlated to the reactive power absorbed by L_p when I_p is maximum; therefore is largely affected by the ratio between the maximum and minimum values of M.

IV. TRACK-SIDE CURRENT CONTROL

Let us control the current in the track side while keeping the current in the pickup side constant at nominal value I_{pN}. This entails that emf in the pickup side must be kept constant and equal to nominal value V_{pN}, i.e. to

$$V_{pN} = \frac{P_{VN}}{I_{pN}} \tag{30}$$

Current I_{pN} is selected in order that V_{pN} meets the relationship

$$V_{pN} = aV_B \tag{31}$$

so that, apart from the possible regulation of the pickup-side current, the chopper remains idle and, in principle, can be removed.

A) Current and voltage relationhips

To keep voltage V_p constant at V_{pN}, current I_t is controlled inversely to M as plotted in Fig. 4. In turn, being I_p constant, voltage V_t increases linearly with M, and the same must happen for V_s. It follows that

$$I_t = \frac{V_{PN}}{\omega M} \tag{32}$$

$$V_s = \omega M I_{pN} \tag{33}$$

Note that the product of I_t by V_s gives P_{VN}, as anticipated. By (30) and (31), current I_t and voltage V_s can be written as

$$I_t = \frac{aV_B}{\omega M} \tag{34}$$

$$V_s = \frac{\omega M P_{VN}}{aV_B} \tag{35}$$

and the maxima of I_t and V_s are

$$\max[I_t] = \frac{aV_B}{\omega M_m} \tag{36}$$

$$\max[V_s] = \frac{\omega M_M P_{VN}}{aV_B} \tag{37}$$

Current I_t is controlled as per (34) by adjusting the output voltage of the HF inverter in agreement with (35).

B) Power sizing factors

Voltage supply power sizing factor. Voltage supply works at variable voltage and current. Its power sizing factor s_s is then equal to the product of the maximum values of the supply voltage and current, and is given by

$$s_s = \frac{M_M}{M_m} \tag{38}$$

Eq. (38) underlines that it is just the ratio between the maximum

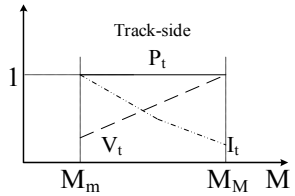

Fig. 4. Track current (dashed-dotted line), voltage (dashed line) and power (solid line) profile under track-side control. Quantities in the graph are normalized to the respective nominal/maximum values.

and minimum values of M.

Pickup power sizing factor. For the EV bus drawing constant power P_{VN}, the terminal voltage of the pickup is constant and is given by

$$V_{pt} = \sqrt{V_{pN}^2 + \left(\omega L_p I_{pN}\right)^2} \tag{39}$$

By applying (10), the sizing factor of the pickup is

$$s_{Lp} = \sqrt{1 + \left(\frac{\omega L_p I_{pN}^2}{P_{VN}}\right)^2} \tag{40}$$

In a dual way to the previous control solution, equation (40) underlines that s_{Lp} exceeds 1 of a term correlated to the reactive power absorbed by L_p. When formulated in terms of P_{VN}, V_B and WPF inductive parameters, equation (40) becomes

$$s_{Lp} = \sqrt{1 + \left[\frac{\omega L_p P_{VN}}{(aV_B)^2}\right]^2} \tag{41}$$

By (41), it can be right asserted that s_{Lp} is less under track side current control than under pickup side current control, the scaling ratio being $(M_M/M_m)^2$ if the second term of the argument of the square root in (41) is much greater than 1.

Track coil power sizing factor. For the EV bus drawing constant power P_{VN}, manipulation of (4) by means of (34) and (35) leads to the expression of V_{tt} in (42), which is directly formulated in terms of P_{VN}, V_B and WPT inductive parameters.

$$V_{tt} = \sqrt{\left(\omega M \frac{P_{VN}}{aV_B}\right)^2 + \left(\frac{L_t}{M} aV_B\right)^2} \tag{42}$$

As a function of M, equation (42) has still a bath-tube profile. Taking the derivative of (42) with respect to M and equating the result to zero yields

$$M_d = aV_B \sqrt{\frac{L_t}{\omega P_{VN}}} \tag{43}$$

Since the sign of the derivative is negative for $M<M_d$ and positive for $M>M_d$, voltage V_{tt} is minimum for $M=M_d$. By (30) and (31), equation (43) can be rewritten in the form

$$M_d = \sqrt{L_t L_p} \sqrt{\frac{aV_B}{\omega L_p I_{pN}}} \tag{44}$$

The first factor in the right-hand side of (44) is equal to M_M/k, where k is the coupling coefficient between the track coil and the pickup. In the practical cases, it is $k<0.3$ so that $\sqrt{L_t L_p}$ is quite greater than M_M. In turn, the second factor in the right-hand side of (44) can be lower than 1 so that the position of M_d depends on the WPF data; consequently, it is not possible to determine a priori whether V_{tt} reaches its maximum value at $M=M_M$ or at $M=M_m$. In the first case, max $[V_{tt}]$ is given by (45) while in the second case it is given by (46).

$$\max[V_{tt}] = \sqrt{\left(\frac{\omega M_M P_{VN}}{aV_B}\right)^2 + \left(\frac{L_t}{M_M} aV_B\right)^2} \tag{45}$$

$$\max[V_{tt}] = \sqrt{\left(\frac{\omega M_m P_{VN}}{aV_B}\right)^2 + \left(\frac{L_t}{M_m} aV_B\right)^2} \tag{46}$$

According to (45) and (46), the power sizing factor of the track coil takes the following expressions:

$$s_{Lt} = \left(\frac{M_M}{M_m}\right) \sqrt{1 + \left[\frac{L_t}{M_M} \frac{(aV_B)^2}{\omega M_M P_{VN}}\right]^2} \tag{47}$$

$$s_{Lt} = \sqrt{1 + \left(\frac{M_M}{M_m}\right)^4 \left[\frac{L_t}{M_M} \frac{(aV_B)^2}{\omega M_M P_{VN}}\right]^2} \tag{48}$$

By (47) and (48), it can be right asserted that s_{Lt} under track side current control is higher than under pickup side current control; when (47) holds, it is M_M/M_m times higher whilst, when (48) holds, it becomes $(M_M/M_m)^2$ times higher if the second term of the argument of the square root in (22) is much greater than 1.

V. POWER SIZING FACTOR COMPARISON

The equations found for the power sizing factors of the voltage supply, the track coil and the pickup under the two control solutions are summarized in Tab. I.

A) Voltage supply power sizing factor

It is readily recognized that the track side current control penalizes the sizing factor of the voltage supply. The penalization degree is exactly given by the ratio M_M/M_m between the maximum and minimum values of M in the WPF operating interval.

B) Track coil and pickup power sizing factors

The track side current control penalizes the power sizing factor of the track coil. The penalization degree varies from a minimum value of M_M/M_m to a maximum value of $(M_M/M_m)^2$, depending on the WPF data. For a given value of M_M/M_m, the penalization degree goes close to the minimum value if the battery voltage is low and the power drawn by EV is high.

In turn, the pickup side current control penalizes the pickup power sizing factor. The penalization degree goes up to $(M_M/M_m)^2$ and, differently from the power sizing factor of the

TABLE I. POWER SIZING FACTOR SUMMARY

	s_{Lp}	s_{Lt}	s_s
Pickup side current control	$\sqrt{1 + \left(\frac{M_M}{M_m}\right)^4 \left[\frac{\omega L_p P_{VN}}{(aV_B)^2}\right]^2}$	$\sqrt{1 + \left[\frac{L_t}{M_M} \frac{(aV_B)^2}{\omega M_M P_{VN}}\right]^2}$	1
Track side current control (maximum of V_{tt} at M_m)	$\sqrt{1 + \left[\frac{\omega L_p P_{VN}}{(aV_B)^2}\right]^2}$	$\left(\frac{M_M}{M_m}\right) \sqrt{1 + \left[\frac{L_t}{M_M} \frac{(aV_B)^2}{\omega M_M P_{VN}}\right]^2}$	$\frac{M_M}{M_m}$
Track side currentcontrol (maximum of V_{tt} at M_M)		$\sqrt{1 + \left(\frac{M_M}{M_m}\right)^4 \left[\frac{L_t}{M_M} \frac{(aV_B)^2}{\omega M_M P_{VN}}\right]^2}$	

track coil, is less if the battery voltage is high and the power drawn by EV is low.

C) General rule

As a general rule, the findings above show that the components in the side where the current control is executed have a higher power sizing.

D) Case study results

The equations developed in the previous Sections are here used to calculate the power sizing factors for the case study of WPF devoted to feed an in-motion C class car. The aim is to quantify the power sizing factors by way of example. The WPF data are reported in the Appendix while the resulting sizing factors are reported in Tab. II. From the WPF data, it comes out that M_d is greater than M_M so that V_{tt} is maximum at $M=M_m$ for both the control solutions; for the sake of completeness, the power sizing factor of the track coil, calculated if voltage V_{tt} would reach the maximum at $M=M_M$, is also given. Inspection of the table points out the huge value of the power sizing factor for the pickup under pickup side current control. It far exceeds the overall power sizing of WPF under track side current control, thus suggesting the convenience of this control solution.

TABLE II. CASE STUDY POWER SIZING FACTORS

	s_{Lp}	s_{Lt}	s_s
Pickup side current control	42.7	2.5	1
Track side current control (maximum of V_{tt} at M_m)	4.8	21	3
Track side current control (maximum of V_{tt} at M_M)		7.6	

VI. CONCLUSIONS

The paper has dealt with WPFs of lumped type, intended to feed in-motion EVs at constant power along a large part of the coupling interval by adjusting the WPF currents. The power sizing of the three key WPF components (voltage supply, track coil and pickup) has been formulated in terms of EV nominal power, EV battery voltage and WPF inductive parameters, including the selectable minimum value of the mutual inductance for the power to be transferred. Two adjustment solutions for the WPF currents have been examined: control of the current either in the pickup side or in the track side, and regulation of the current in the other side. The equations found have clearly demonstrated that the power sizing is higher for the WPF components placed in the side where the current control is executed.

Power sizing of the WPF components is a measure of their cost and volume. From this perspective, the equations of the component power sizing assist a designer in stressing the impact of WPF on EVs and the infrastructure builders. For instance, the track side current control keeps lower the power sizing of the pickup which makes it less expensive and more appropriate for space demanding applications like those on-board EVs. On the other side, such a control calls for a higher power sizing of the voltage supply and the track coils, which appears a more reasonable allocation by accounting that they are installed on the road.

APPENDIX

The case study examined in Section V refers to WPF of lumped type designed to feed in-motion electric cars [14]. Data of WPF are: supply frequency of 85 kHz, both coil self-inductances of 18.3 μH, and coupling coefficient of 0.3, which means that M_M is equal to 5.5 μH. Data of the cars are: on-board battery of 360 V/36 kWh, and average drawn power of 34 kW when cruising at the constant speed of 120 km/h. By imposing that V_{CH} at $M=M_M$ is equal to battery voltage (i.e. to 360 V), it follows that V_{pN} is equal to 328 V and V_{tN} to 537 V. For a track with side-by-side coupling intervals and a value of M_m set at $M_M/3$, the power to be transferred along the WPF operating interval is of 51 kW, being such an interval equal to 2/3 of the coupling interval.

REFERENCES

[1] D.Patil, M.K.McDonough, J.M.Miller, B.Fahimi and P.T. Balsara, "Wireless Power Transfer for Vehicular Applications: Overview and Challenges," *IEEE Trans. on Transportation Electrification*, vol. 4, no. 1, pp. 3-37, March 2018.

[2] C.C.Mi, G. Buja, S.Y.Choi, and C.T.Rim, "Modern Advances in Wireless Power Transfer Systems for Roadway Powered Electric Vehicles", *IEEE Trans. on Industrial Electronics*, vol. 63, no. 10, pp. 6533-6545, Oct 2016.

[3] J.Lukic and Z. Pantic, "Cutting the cord: Static and dynamic inductive wireless charging of electric vehicles," *IEEE Electrification Magazine*, vol. 1, no. 1, pp. 57–64, Sep. 2013.

[4] L. Hutchinson, B. Waterson, B. Anvari and D. Naberezhnykh, "Potential of wireless power transfer for dynamic charging of electric vehicles," *IET Intelligent Transport Systems*, vol. 13, no. 1, pp. 3-12, 1 2019.

[5] J. M. Miller, O. Onar, C.White, C.Campbell, C.Coomer, L.Seiber, R.Sepe, and A.Steyerl, "Demonstrating Dynamic Wireless Charging of an Electric Vehicle: The Benefit of Electrochemical Capacitor Smoothing," *IEEE Power Electronics Magazine*, vol. 1, no. 1, pp. 12–24, Mar. 2014.

[6] Z.Zhang and K.Chau, "Homogeneous wireless power transfer for move and-charge," *IEEE Trans. on Power Electronics*, vol. 30, no. 11, pp. 6213–6220, Nov. 2015.

[7] K.Lee, Z.Pantic, and S.M.Lukic, "Reflexive field containment in dynamic inductive power transfer systems," *IEEE Trans. on Power Electronics*, vol. 29, no. 9, pp. 4592–4602, Sep. 2014.

[8] M.Borage, S.Tiwari, and S.Kotaiah, "LCL-T Resonant Converter With Clamp Diodes: A Novel Constant-Current Power Supply With Inherent Constant-Voltage Limit," *IEEE Trans. on Industrial Electronics*, vol. 54, no. 2, pp. 741-746, April 2007.

[9] J.Acero, C.Carretero, I.Lope, R.Alonso, O.Lucia, and J.M.Burdio, "Analysis of the mutual inductance of planar-lumped inductive power transfer systems," *IEEE Trans. on Industrial Electronics*, vol. 60, no. 1, pp. 410–420, Jan. 2013.

[10] J. L.Villa, J.Sallan, J. F.Sanz Osorio, and A.Llombart, "High misalignment tolerant compensation topology for ICPT systems," *IEEE Trans. on Industrial Electronics*, vol. 59, no. 2, pp. 945–951, Feb. 2012.

[11] H.Feng, T.Cai, S.Duan, J.Zhao, X.Zhang, and C.Chen, "An LCC-Compensated Resonant Converter Optimized for Robust Reaction to Large Coupling Variation in Dynamic Wireless Power Transfer," *IEEE Trans. on Industrial Electronics*, vol. 63, no. 10, pp. 6591-6601, Oct. 2016.

[12] J.Zhao, T.Cai, S.Duan, H.Feng, C.Chen, and X.Zhang, "A General Design Method of Primary Compensation Network for Dynamic WPT System Maintaining Stable Transmission Power," *IEEE Trans. on Power Electronics*, vol. 31, no. 12, pp. 8343-8358, Dec. 2016.

[13] M.Bertoluzzo, R.Jha, and G.Buja, "Power Transfer Profile Boosting in DWC Systems by Two-Element Compensation Network", Proc. of IEEE PELS Workshop on Emerging Technologies: Wireless Power, pp. 1-6, 2019.

[14] G.Buja, M.Bertoluzzo and H.K.Dashora, "Lumped Track Layout Design for Dynamic Wireless Charging of Electric Vehicles," *IEEE Trans. on Industrial Electronics*, vol. 63, no. 10, pp. 6631-6640, Oct. 2016.